TECHNICAL NOTES

NATIONAL ADVISORY COMMITTEE FOR AERONAUTICS

No. 835

ANALYSIS OF GROUND EFFECT ON THE LIFTING AIRSCREW

By Montgomery Knight and Ralph A. Hefner
Daniel Guggenheim School of Aeronautics
Georgia School of Technology

Washington
December 1941

NATIONAL ADVISORY COMMITTEE FOR AERONAUTICS

TECHNICAL NOTE NO. 835

ANALYSIS OF GROUND EFFECT ON THE LIFTING AIRSCREW

By Montgomery Knight and Ralph A. Hefner

SUMMARY

A study is presented of ground effect as applied to the lifting airscrew of the type used in modern gyroplanes and helicopters. The mathematical analysis of the problem has been verified by tests made of three rotor models in the presence of a large circular "ground plane." A method of approximating the decelerating effect during vertical approach to the ground has been devised. The results of the study are presented in the form of convenient charts.

INTRODUCTION

Proximity to the ground has a pronounced effect on the aerodynamic characteristics of the lifting airscrew. Ground effect is therefore of importance in the study of the landing and the take-off qualities of gyroplanes and helicopters. No comprehensive attack on this problem has thus far been found by the writers although it has been mentioned occasionally in the literature (references 1, 2, and 3), and an approximate mathematical analysis has been made by Betz (reference 4).

The investigation described in this report was undertaken to obtain a general solution of the problem of ground effect on the lifting airscrew. It constitutes a portion of a broad program of research on the lifting airscrew that was instituted several years ago at the Georgia School of Technology.

The investigation consisted of a mathematical analysis of ground effect, the validity of which was verified by tests of three lifting airscrew models operating in proximity to a large, circular ground plane. A method of approximating the decelerating effect on a lifting rotor during vertical approach to the ground was also devised and is presented in the appendix.

The present investigation was conducted by the staff of the Guggenheim Aeronautics Division of the State Engineering Experiment Station and has been financed in part by the National Advisory Committee for Aeronautics. The writers wish to acknowledge the valuable aid of Messrs. R. H. Fagan and L. I. Turner in conducting the model tests, and the excellent work of Mr. W. C. Slocum in constructing the models and ground plane.

MATHEMATICAL ANALYSIS

In the approach to the problem of ground effect from the mathematical standpoint, it was decided that application of the reflection method to the static-thrust analysis as developed in reference 5 offered the greatest possibilities. The complexity of the mathematical analysis made expedient the following assumptions:

1. The number of blades could be taken as infinite.

2. The usual angle approximations could be made because all angles associated with the induced velocity were small.

3. Rotational and radial components of velocity and tip effects could be neglected.

4. The slipstream contraction could be neglected.

These assumptions are now generally used in lifting-airscrew analyses. It was discovered, however, that the principle of the aerodynamic independence of blade elements (reference 5) is no longer valid when the airscrew is near the ground; hence an exact general solution for ground effect is practically impossible. An approximate solution was reached by the expedient of specifying, for analytical purposes, that the circulation along the airscrew blades be constant, that is, independent of both the radius and the distance above the ground.

If the rotating blades are twisted in such a manner as to keep the circulation along them constant, there are trailing vortices only at the tips and the roots of the blades. For a rotor with infinitely many blades, the trailing tip vortices form a cylindrical sheet of vorticity of strength k per unit length.

When the rotor is a distance Z above the ground, the effect may be represented by placing a second cylindrical vortex sheet of equal length and strength but of opposite direction at the end of the first cylinder as shown in figure 1. The first cylinder, which is associated with the actual airscrew, is thus mirrored by the second.

Induced Velocity

In reference 5 it was shown that the axial induced velocity at a point due to a cylindrical vortex sheet was equal to $\frac{1}{4\pi}\frac{d\Gamma}{dZ}$ times the difference in the solid angles subtended by the ends of the cylinder. Thus, for a point P (fig. 1) the induced velocity in the Z-direction due to cylinder A is

$$w_A = (2\pi - \alpha)\frac{k}{4\pi}$$

$$k = \frac{d\Gamma}{dZ}$$

where

Γ = circulation

α = solid angle at P subtended by ground trace of rotor

The induced velocity due to cylinder B is

$$w_B = -(\alpha - \beta)\frac{k}{4\pi}$$

where β is the solid angle at P subtended by the reflection of the rotor. Adding these two velocities, the induced velocity in the Z-direction at point P is found to be

$$w = (2\pi - 2\alpha + \beta)\frac{k}{4\pi}$$

Letting $x = r/R$, $l = Z/R$, and setting up the integrals for these solid angles,

$$w = \frac{kl}{\pi}\int_0^{\pi} \frac{1 - x\cos\theta}{x^2 + 1 - 2x\cos\theta}\left[\frac{1}{\sqrt{l^2 + x^2 + 1 - 2x\cos\theta}} - \frac{1}{\sqrt{4l^2 + x^2 + 1 - 2x\cos\theta}}\right] d\theta \qquad (1)$$

On reducing these elliptic integrals to standard form,

$$w = \frac{kl}{\pi\sqrt{l^2(1+x)^2}}\left[F\left(\sqrt{\frac{4x}{l^2 + (1+x)^2}}\right) + \left(\frac{1 - x}{1 + x}\right)\Pi\left(\frac{-4x}{(1+x)^2}, \sqrt{\frac{4x}{l^2 + (1+x)^2}}\right)\right]$$

$$- \frac{kl}{\pi\sqrt{4l^2 + (1+x)^2}}\left[F\left(\sqrt{\frac{4x}{4l^2 + (1+x)^2}}\right) + \left(\frac{1 - x}{1 - x}\right)\Pi\left(\frac{-4x}{(1+x)^2}, \sqrt{\frac{4x}{4l^2 + (1+x)^2}}\right)\right] \qquad (2)$$

where F and Π are complete elliptic integrals of the first and the third kinds, respectively.

When the point P is in the center of the cylinder, $x = 0$, and w reduces to

$$w_c = kl\left[\frac{1}{\sqrt{l^2 + 1}} - \frac{1}{\sqrt{4l^2 + 1}}\right] \qquad (3)$$

When the point P is at the tip of the blade, $x = 1$, but the expression in equation (2) for w becomes indeterminate. Going back to equation (1), setting $x = 1$, and then integrating, the induced velocity at the tip becomes

$$w_t = \frac{kl}{\pi\sqrt{l^2 + 4}} F\left(\frac{2}{\sqrt{l^2 + 4}}\right) - \frac{kl}{2\pi\sqrt{l^2 + 1}} F\left(\frac{1}{\sqrt{l^2 + 1}}\right) \qquad (4)$$

This expression turns out to be the result that would

be obtained from equation (2) if $x = 1$, and it is assumed that the indeterminate value $0 \times \infty$, which arises, is zero.

For this particular indeterminate form, however, the two variables involved are independent, and the indeterminate form cannot be evaluated by the usual methods. Equation (4) is the value obtained when x approaches its limit first and is not the value desired. The value required is obtained when θ approaches its limit first, and then x approaches its liniting value. This value is different from that obtained in equation (4).

In order to find the difference in the two methods, consider figure 1. If r approaches R from either side, it is obvious that the solid angles α and β are both continuous and approach the value they have when $r = R$. On the other hand, the solid angle of the rotor disk itself, as r approaches R from the inside, is a constant and is equal to 2π. The solid angle of the rotor disk when $r = R$ is π and, when r approaches R from the outside, the solid angle is zero.

Let

(w_t^+) induced velocity approached at tip from inside

(w_t) induced velocity at the tip

(w_t^-) induced velocity approached at tip from outside

Then, when $r = R$,

$$(w_t) = \frac{\pi - 2\alpha + \beta}{4\pi} k$$

$$(w_t^+) = \frac{2\pi - 2\alpha + \beta}{4\pi} k$$

$$(w_t^-) = \frac{\beta - 2\alpha}{4\pi} k$$

From these expressions, it can be seen at once that

$$(w_t^+) = (w_t) + 0.25\ k$$

$$(w_t^-) = (w_t) - 0.25\ k$$

Thus, both (w_t^+) and (w_t^-) can easily be computed by using equation (4). Curves of (w_c/k) and (w_t^+/k) against Z/R are given in figure 2.

When the point P is somewhere between the center and the tip $(0 < x < 1)$, it is extremely tedious and difficult to compute the induced velocity with a high degree of accuracy if equation (2) is used. This difficulty is due to the presence of the elliptic integral of the third kind for which no tables are available. Thus, the exact solution is found to be of no practical value.

Methods of Approximation

Two methods of approximating the induced velocity between the extreme values may be used. The first method is to approximate the integral in equation (1) by Simpson's rule. This method yielded a satisfactory degree of accuracy for values of Z/R up to 2 except near the tip. As $r \longrightarrow R$, and for values of $Z/R > 2$, it was found impossible to determine w with any degree of accuracy without computing a prohibitive number of ordinates.

In order to obtain an expression that could be used for the larger values of Z/R, the induced velocity was expressed as an infinite series of Legendre's polynomials.

Let C (fig. 3) be a circular vortex ring of strength Γ, the center of which is taken to be the origin of a system of polar coordinates. (Note that small r in fig. 3 is a different r than shown in fig. 1.)

The potential at any point P due to this vortex ring is

$$\Phi = \frac{\Gamma}{4\pi} w$$

where w is the solid angle subtended at P by the ring.

If $\theta = 0$, the point P is on the axis of the circle and

$$w = 2\pi \left(1 - \frac{r}{\sqrt{a^2 + r^2}}\right)$$

Hence

$$\Phi = \frac{\Gamma}{2}\left(1 - \frac{r}{\sqrt{a^2 + r^2}}\right)$$

Expanding in powers of r by the binomial theorem,

$$\Phi = \frac{\Gamma}{2} \sum_{n=1}^{\infty} \frac{(-1)^{n+1} \underline{/2n-1}}{2^{2n-1} \underline{/n} \, \underline{/n-1}} \left(\frac{a}{r}\right)^{2n} \qquad (5)$$

which converges for all values of r greater than a. From this result it is possible to deduce the potential at any point in space outside a sphere whose radius is a.

The potential sought is a solution of the equation $\Delta^2 \Phi = 0$ and is symmetrical about the θ-axis. The solution is therefore capable of being expressed as an infinite series of the form

$$\Phi = \sum_{n=1}^{\infty} B_n \frac{1}{r^n} P_n (\cos \theta) \quad \text{if } r > 1 \qquad (5a)$$

where the B's are constants and the $P_n(\cos\theta)$ terms are Legendre's polynomials.

When $\theta = 0$, $\cos \theta = 1$, $P_n(1) = 1$ and

$$\Phi = \sum_{n=1}^{\infty} B_n \frac{1}{r^n} \quad \text{if } r > 1 \qquad (6)$$

When $\theta = 0$, the point P is on the axis, and equations (5) and (6) must be identical. Equating coefficients, solving for the B's, and substituting them in equation (5a),

$$\Phi = \frac{\Gamma}{2} \sum_{n=1}^{\infty} \frac{(-1)^{n+1} \underline{/2n-1}}{2^{2n-1} \underline{/n} \, \underline{/n-1}} \left(\frac{a}{r}\right)^{2n} P_n (\cos \theta)$$

$$\text{if } r > a \qquad (7)$$

Consider now a cylindrical vortex sheet of strength k per unit length. Let the length of the cylinder be Z and let the Z-axis of a rectangular set of axes be the axis of the cylinder (fig. 4). Furthermore, let the near end of the

cylinder be b units from the origin and let b be greater than the radius R.

Consider an elementary section of the cylinder of length dZ. Since the strength per unit length is k, $k = d\Gamma/dZ$, and the strength of the elementary section dZ is

$$\frac{d\Gamma}{dZ}\,dZ = k\,dZ$$

If the strength is considered to be concentrated along the circle splitting the center of the elementary section, the differential of the potential at the point P can be found by using equation (7), and

$$d\Phi = \frac{k}{2}\sum_{n=1}^{\infty}\frac{(-1)^{n+1}\,\underline{/2n-1}}{2^{2n-1}\,\underline{/n}\,\underline{/n-1}}\left(\frac{R}{\sqrt{Z^2+a^2}}\right)^{2n} P_{2n}\left(\cos\tan^{-1}\frac{a}{Z}\right)dZ \tag{8}$$

The series in equation (8) converges if $\sqrt{Z^2 + a^2} > R$ and, since $b > R$, the series converges over the entire cylinder.

The potential at point P due to the entire cylinder is therefore

$$\Phi = \int_{z_1+b}^{b}\frac{d\Phi}{dZ}\,dZ$$

But the induced velocity in the Z-direction due to the cylindrical vortex is

$$w = \frac{\partial\Phi}{\partial Z} = \frac{\partial\Phi}{\partial Z}\Bigg]_{z_1+b}^{b}$$

To simplify the expression for w, let

$$\psi(Z) = \frac{k}{2}\sum_{n=1}^{\infty}\frac{(-1)^{n+1}\,\underline{/2n-1}}{2^{2n-1}\,\underline{/n}\,\underline{/n-1}}\left(\frac{R^2}{Z^2+a^2}\right)P_{2n}\left(\cos\tan^{-1}\frac{a}{Z}\right)$$

Then

$$w = \frac{\partial\Phi}{\partial Z}\Bigg]_{z_1+b}^{b} = \psi(b) - \psi(Z+b) \tag{9}$$

which is valid as long as $b > R$.

It is important to note that at P (fig. 4) w is equal to the difference in the potentials due to the two ends of the cylinder if they are considered to be vortex rings of strength k. Hence, it is clear that the induced velocity in the Z-direction at a point in the end of a cylindrical vortex of length $Z_1 > R$ is

$$w = \frac{k}{2} - \psi(Z_1) \tag{10}$$

Hence, the ground effect on the induced velocity at any point in the rotor is the difference between equations (10) and (9) when both Z_1 and b are replaced by Z. Thus

$$w = \frac{k}{2} - 2\,\psi(Z) + \psi(2Z) \quad \text{if} \quad Z > R \tag{11}$$

Let $l = \frac{Z}{R}$

$x = \frac{a}{R}$

The first few terms of equation (11) are

$$w = \frac{k}{2}\left\{\left[\frac{1}{2}\left(\frac{1}{4l^2+x^2}\right) P_2(\cos\theta_2) - \frac{3}{8}\left(\frac{1}{4l^2+x^2}\right)^2 P_4(\cos\theta_2) + \frac{5}{16}\left(\frac{1}{4l^2+x^2}\right)^3 P_6(\cos\theta_2)\right] + 1 - 2\left[\frac{1}{2}\left(\frac{1}{l^2+x^2}\right) P_2(\cos\theta_1) - \frac{3}{8}\left(\frac{1}{l^2+x^2}\right)^2 P_4(\cos\theta_1) + \frac{5}{16}\left(\frac{1}{4l^2+x^2}\right)^3 P_6(\cos\theta_1)\right]\right\} \tag{12}$$

where

$$\theta_1 = \tan^{-1}\frac{x}{l}$$

$$\theta_2 = \tan^{-1}\frac{x}{2l} \qquad x < 1, \quad l > 1$$

Equation (12) was used to compute values of w for $l = 2$ and $l = 3$.

The values of w obtained by this second method of approximation were checked against those found by the first method. After cross-plotting and fairing, curves were obtained that represent with a fair degree of accuracy the induced velocity along the blade for various values of Z/R. These curves are given in figure 5.

Thrust

The thrust coefficient is expressed in reference 5 by the integral

$$C_T = a_o \sigma \int_{?}^{1} (\theta - \varphi) x^2 \, dx \qquad (13)$$

where (fig. 6)

a_o slope of lift curve for infinite wing

σ rotor solidity $(Bc/\pi R)$

θ blade incidence

φ induced flow angle

x r/R

B number of blades

c chord of blades

By assumption, the circulation Γ is constant along the blade, and since for constant chord blades (reference 5),

$$\Gamma = \frac{Bc}{2} a_o (\theta - \varphi) \Omega r$$

$$= \frac{Bc}{2} a_o (\theta - \varphi) \Omega R x$$

where Ω is the angular velocity of the rotor.

Thus

$$(\theta - \varphi)\, x = \frac{2\,\Gamma}{Bc\; a_o\; \Omega\; r} = \text{constant} \tag{14}$$

Equation (13) may now be written

$$C_T = a_o\, \sigma(\theta - \varphi)\, x \int_o^1 x\, dx$$

$$= \frac{1}{2}\, a_o\, \sigma(\theta - \varphi)\, x$$

or

$$T_\sigma = \frac{C_T}{\sigma^2} = \frac{1}{2}\, a_o(\theta_\sigma - \varphi_\sigma)\, x \tag{15}$$

Equation (14) shows that the thrust is independent of Z/R on the basis of the assumption that the circulation Γ is constant along the blade and independent of altitude. The thrust can therefore be found from the thrust curves for infinite Z/R obtained in reference 5. Thus, the thrust coefficient may be expressed as

$$T_\sigma = T_{\sigma_o}$$

$$= \frac{1}{2}\, a_o\, (\theta_{\sigma_o} - \varphi_{\sigma_o}) \tag{16}$$

Total Torque

The total torque coefficient of the lifting airscrew may be written (reference 5) as

$$Q_\sigma = Q_{\sigma_i} + Q_{\sigma_\epsilon} + Q_{\sigma_\delta}$$

Q_{σ_i} induced torque coefficient

Q_{σ_ϵ} profile variation torque coefficient

Q_{σ_δ} minimum profile torque coefficient $(\delta/4\sigma^2)$

δ minimum profile drag coefficient of blades

Profile-Variation Torque

The coefficient of profile-variation torque is defined in reference 5 by the integral

$$C_{Q_\epsilon} = \sigma \epsilon \int_0^1 a_0^2 (\theta-\varphi)^2 x^3 \, dx$$

Again by using equation (4),

$$C_{Q_\epsilon} = a_0^2 \frac{\sigma\epsilon}{2} (\theta-\varphi)^2 x^2 \int_0^1 x \, dx$$

$$= \frac{a_0^2 \sigma \epsilon}{2} (\theta - \varphi)^2 x^2$$

$$Q_{\sigma_\epsilon} = \frac{a_0^2 \epsilon}{2} (\theta_{\sigma_0} - \varphi_{\sigma_0})^2$$

$$= 2\epsilon \, T_{\sigma_0}^2$$

Thus profile-variation torque is also independent of Z/R.

Induced Torque

Unlike the profile-variation torque, the induced torque is not independent of Z/R.

In order to compute the induced torque from the induced velocity already determined, it was found expedient to derive a relation between the induced torque, the thrust, and the induced velocity for a single finite cylindrical vortex sheet, and then to specialize the result for the case of the double vortex sheet representing the ground effect.

The induced velocity approached at the tip of the blade for a finite cylindrical vortex sheet is

$$w_0 = \frac{1}{4\pi} \frac{d\Gamma}{dZ} \left[w(Z_2) - w(Z_1) \right]_{x \longrightarrow 1}$$

Solving for $d\Gamma/dZ$

$$\frac{d\Gamma}{dZ} = \frac{4\pi w_0}{\left[w(Z_2) - w(Z_1)\right]_{x \longrightarrow 1}} \tag{17}$$

Now

$$\frac{d\Gamma}{dZ} = \frac{\Gamma}{Bd}$$

where

$$d = \frac{2\pi w_0}{\Omega B}$$

Using these relations, equation (17) becomes

$$\frac{\Omega \Gamma}{2\pi w_0} = \frac{4\pi w_0}{\left[w(Z_2) - w(Z_1)\right]_{x \longrightarrow 1}}$$

Solving this expression for w_0

$$w_0 = \frac{1}{4\pi} \sqrt{2 \Omega \Gamma \left[w(Z_2) - w(Z_1)\right]_{x \longrightarrow 1}}$$

Using this value of w_0, equation (17) becomes

$$\frac{d\Gamma}{dZ} = \sqrt{\frac{2 \Omega \Gamma}{\left[w(Z_2) - w(Z_1)\right]_{x \longrightarrow 1}}} \tag{18}$$

Now the induced velocity anywhere along the blade is given by

$$w = \frac{\frac{d\Gamma}{dZ}}{4\pi} \left[w(Z_2) - w(Z_1)\right]_{x < 1}$$

Using the value of $d\Gamma/dZ$ from equation (18)

$$w = \frac{\sqrt{2\Omega\Gamma}}{4\pi} \left\{ \frac{\left[w(Z_2) - w(Z_1)\right]_{x<1}}{\left[w(Z_2) - w(Z_1)\right]^{1/2}_{x \longrightarrow 1}} \right\} \tag{19}$$

Now

$$\Gamma = Bc \frac{a_0}{2} (\theta - \varphi) \Omega r$$

$$= \frac{Bc}{\pi R} \frac{a_0}{2} (\theta - \varphi) \pi R^2 \Omega x$$

$$\Gamma = \sigma^2 \frac{a_o}{2} (\theta_\sigma - \varphi_\sigma) \pi R^2 \Omega x$$

$$= \sigma^2 \pi \Omega R^2 T_\sigma$$

Placing this value of Γ in equation (19)

$$w = \frac{\sigma \Omega R T_\sigma^{1/2}}{\sqrt{8\pi}} \left\{ \frac{[w(Z_2) - w(Z_1)]_{x<1}}{[w(Z_2) - w(Z_1)]^{1/2}_{x \to 1}} \right\} \qquad (20)$$

The induced torque is given by the expression

$$Q_i = \frac{\rho}{2} Bc\, a_o \int_0^R (\theta - \varphi)\, r\, \varphi\, \Omega^2\, r^2\, dr$$

$$= \frac{\rho}{2} Bc\, a_o R^4 \int_0^1 (\theta - \varphi)\, x\, \varphi\, \Omega^2\, x^2\, dx$$

Since by equation (14), $(\theta - \varphi)\, x$ is a constant,

$$Q_i = \frac{\rho}{2} Bc\, a_o\, (\theta - \varphi)\, x\, R^4 \int_0^1 \varphi\, \Omega^2\, x^2\, dx$$

or

$$Q_{\sigma_i} = \frac{2\sigma \frac{a_o}{2} (\theta - \varphi)\, x}{\Omega R \sigma^3} \int_0^1 w\, x\, dx$$

Using equation (15),

$$Q_{\sigma_i} = \frac{2 T_\sigma}{\sigma \Omega R} \int_0^1 w\, x\, dx$$

Using the value of w found in equation (20),

$$Q_{\sigma_i} = \frac{T_\sigma^{3/2}}{\sqrt{2\pi} \left[w(Z_2) - w(Z_1) \right]^{1/2}_{x \to 1}} \int_0^1 \left\{ \left[w(Z_2) - w(Z_1) \right]_{x<1} \right\} x\, dx \qquad (21)$$

In the case of ground effect, instead of the induced velocity merely being proportional to the difference in the solid angles $w(Z_2)$ and $w(Z_1)$ as in reference 5, a more

complex relationship exists. In order to change equation (21) so that it represents ground effect, replace $[w(Z_2) - w(Z_1)]$ by $[w(Z/R,x)/k]\ 4\pi$ where $w(Z/R,x)$ is the function given by equation (1).

Hence, in the case of ground effect,

$$Q_{\sigma_i} = \frac{\sqrt{2}\ T_\sigma^{3/2}}{\left[\frac{w\left(\frac{Z}{R},1\right)^+}{k}\right]^{1/2}} \int_0^1 \frac{w\left(\frac{Z}{R},x\right)}{k}\ x\ dx$$

If

$$f\left(\frac{Z}{R}\right) \equiv \sqrt{\frac{2k}{w\left(\frac{Z}{R},1\right)^+}} \int_0^1 \frac{w\left(\frac{Z}{R},x\right)}{k}\ x\ dx$$

Then

$$Q_{\sigma_i} = f\left(\frac{Z}{R}\right) T_\sigma^{3/2}$$

or

$$Q_{\sigma_i} = f\left(\frac{Z}{R}\right) T_{\sigma_o}^{3/2}$$

since the thrust is constant.

A convenient method of expressing ground effect is to plot the change of torque coefficient against altitude for the condition of constant thrust coefficient. The use of the coefficient (reference 5),

$$Q_\sigma' = Q_\sigma - Q_{\sigma_{min}}$$
$$= Q_{\sigma_i} + Q_{\sigma_\epsilon}$$

gives the simplest result.

The analysis has shown that

$$Q_\sigma' = f\left(\frac{Z}{R}\right) T_{\sigma_o}^{3/2} + 2\epsilon\ T_{\sigma_o}^2$$

and

$$Q_{\sigma_o}' = \frac{1}{2}\ T_{\sigma_o}^{3/2} + 2\epsilon\ T_{\sigma_o}^2$$

for

$$Z/R = \infty$$

The change in torque may thus be written as

$$\Lambda = \frac{Q_{\sigma}'}{Q_{\sigma_o}'}$$

$$= \frac{f\left(\frac{Z}{R}\right) + 2\epsilon\, T_{\sigma_o}^{1/2}}{\frac{1}{2} + 2\epsilon\, T_{\sigma_o}^{1/2}}$$

and this parameter is given in figure 7 for a range of values of T_{σ_o}.

EXPERIMENTAL DATA

In order to verify the foregoing mathematical analysis, tests on three rotor models were made in the presence of a large, circular ground plane. These tests were made in the open throat of the Georgia School of Technology 9-foot wind tunnel.

Rotor Models

Three rotor models with two, three, and four blades, respectively, and a diameter of 5 feet were used. The same models had been employed previously in the static-thrust tests (reference 5). Each blade had the NACA 0015 profile and a chord of 2 inches from the 5-inch radius to the tip. There was no twist. The blades were hinged horizontally at a radius of 1 inch and were balanced about the quarter-chord line, which intersected the axis of rotation. The blade incidence was adjustable.

Test Apparatus

The method of mounting the models and measuring the forces is described in reference 5. An improved drive, however, was used in the present tests. It consisted of a 1-horsepower, three-phase synchronous motor driving the model through gearing and shafts. Thus, the model speed was constant within small limits at 900 rpm because the frequency variations in the line were negligible.

The ground plane consisted of a disk of 1/4-inch plywood, 12 feet in diameter, generously reinforced at the back as shown in figure 8. It was mounted so as to slide on a steel tube suspended by cables. A spring-operated pin engaged holes in the tube to lock the plane in position with respect to the rotor, which was turned into the tunnel downwind direction, as shown. This arrangement permitted a range of distances from 0.25 to 2.20 in terms of the rotor radius to be used. Figure 9 shows the set-up with the three-blade rotor as viewed from the entrance cone of the tunnel.

The test procedure consisted of setting the blades of the model at a given angle using the incidence jig described in reference 5. The rotor was then mounted in the tunnel, and the thrust and the torque were measured for each position of the ground plane.

The experimental data thus obtained were reduced to the nondimensional forms used in the mathematical analysis with the aid of the following equations:

$$T_\sigma = \frac{2T}{\rho \pi R^2 \Omega^2 R^2 \sigma^2}$$

$$Q_{\sigma'} = Q_\sigma - Q_{\sigma_{min}}$$

$$\sigma' = \frac{2(Q - Q_{min})}{\rho \pi R^2 \Omega^2 R^3 \sigma^3}$$

where Q_{min} is the measured torque where $\theta = 0$.

RESULTS AND DISCUSSION

A comparison of the results of the tests with those of the mathematical analysis is presented in figure 10. In each of the sections of figure 10 the curve of $Q_{\sigma'}$ against T_σ for $Z/R = \infty$ is plotted as obtained from table I of reference 5. The values of the torque coefficient for $Z/R = 0.25$, 0.50, 1.00, 1.50, and 2.00 have been computed from the relationship

$$Q_{\sigma'} = \Lambda Q_{\sigma_o'}$$

where the appropriate values of Λ have been obtained from figure 7. These curves of Q_σ' are also drawn in the figures, and the test points are spotted in for comparison.

It will be noted from these figures that the agreement between the experimental and the analytical values of Q_σ' is quite good except for $Z/R = 0.25$ and 0.50 where, as might be expected, the rotor blades begin to stall at the larger angles because of the sharp reduction in induced velocity. This stalled condition was, of course, accentuated by the low Reynolds number at which the blades were operating during the tests.

The agreement between the experimental and the analytical results is all the more notable in that the distribution of circulation along the blades is entirely different for the two cases. Even large changes of distribution appear, however, to produce only slight changes in total thrust and torque, as is generally true of airscrews.

Inspection of tables I to III shows that, for constant-chord, constant-incidence rotor blades, the torque coefficient changes very little at distances from the ground greater than $Z/R = 0.50$. This form of airscrew might, therefore, be termed the "constant-torque" type in contradistinction to the hypothetical "constant-thrust" type used in the theory.

Evidently then, the constant-torque rotor will experience a change in thrust as it approaches the ground. An approximate representation of this thrust variation is given in figure 11, which was obtained by cross-plotting the curves of figure 10 for constant values of Q_σ'.

CONCLUSIONS

The following conclusions may be arrived at as a result of this investigation:

1. On the assumption that the circulation around the blades of a lifting airscrew is independent of radius and ground distance, the variation in induced velocity due to ground effect may be set up either as an elliptic integral or as a series of Legendre's polynomials.

2. Ground effect on the thrust and the torque of a lifting airscrew rapidly decreases with altitude, becoming practically negligible at a height equal to the rotor diameter.

3. The ground-effect test data obtained on the constant-chord, constant-incidence rotor models show satisfactory agreement with the calculated results.

4. These tests also indicate that the torque coefficient is substantially constant except at very small heights above the ground but that there is a large thrust-coefficient increase as the rotor approaches the ground.

5. It is possible to arrive at an approximate theoretical determination of the thrust-coefficient variation with ground distance for conventional constant-incidence rotors by using the constant-torque-coefficient condition.

Daniel Guggenheim School of Aeronautics,
Georgia School of Technology,
Atlanta, Georgia, May 29, 1940.

APPENDIX

Deceleration Due to Ground Effect

An important application of ground effect is its use in the vertical landing approach of a helicopter. The decelerations thus experienced can be shown to be sufficiently large to afford a method of landing such an aircraft automatically and without appreciable shock.

The general equation of motion of a helicopter in vertical descent is

$$m\,a = T - W \tag{1}$$

where

a acceleration

m mass of machine

W weight of machine

T thrust

This equation will have the following forms:

$$\frac{W}{g}\frac{d^2Z}{dt^2} = T - W$$

or

$$\frac{dV}{dt} = \frac{g}{W}(T - W) \tag{2}$$

where

V velocity of vertical descent

Z vertical distance above ground

t time

Equation (2) may be written

$$\frac{dV}{dZ}\frac{dZ}{dt} = \frac{g}{W}(T - W)$$

or
$$V\,dV = g\left(\frac{T}{W} - 1\right) dZ \tag{3}$$

In steady descent at altitudes greater than $Z/R = 2.0$, the initial thrust, T_o, may be taken as equal to the weight W, and so

$$V\,dV = g\left(\frac{T}{T_o} - 1\right) dZ \tag{4}$$

$$= g\,R\left(\frac{T}{T_o} - 1\right) d\zeta \tag{5}$$

where

$$\zeta = \frac{Z}{R}$$

Integrating both sides of equation (5),

$$\frac{1}{gR}\int_{V_o}^{V} V\,dV = \int_{\zeta_o}^{\zeta} \frac{T_\sigma}{T_{\sigma_o}}\,d\zeta - \int_{\zeta_o}^{\zeta} d\zeta$$

or

$$\frac{V^2 - V_o^2}{2g\,R} = \int_{\zeta_o}^{\zeta} \frac{T_\sigma}{T_{\sigma_o}}\,d\zeta - \zeta + \zeta_o \tag{6}$$

where

V_o initial vertical velocity

ζ_o altitude ratio at which ground effect becomes appreciable

More conveniently

$$\left(\frac{V}{V_o}\right) = \sqrt{1 - \frac{2gR}{V_o^2}\left[\zeta - \zeta_o + \int_{\zeta}^{\zeta_o} \frac{T_\sigma}{T_{\sigma_o}}\,d\zeta\right]} \tag{7}$$

The special case of $V = 0$ at $\zeta < \zeta_o$ is of interest because it represents the condition of landing without shock. For this case, equation (6) becomes

$$V_o = \sqrt{2gR\left[l - l_o \int_{l}^{l_\infty} \frac{T_\sigma}{T_{\sigma_o}} \, dl\right]} \qquad (8)$$

An exact solution of equations (7) and (8) is impossible at present, because the exact form of $T_\sigma/T_{\sigma_o} = f(l)$ is not known for vertical descent in proximity to the ground. An approximate solution is, however, possible.

It will be noted in figure 11 that the effect of changes in Q_σ' on the ratio T_σ/T_{σ_o} is not large. In addition, a recent investigation (reference 6) on helicopter vertical motion conducted at this institution has indicated that, for rates of vertical descent up to 20 feet per second, the changes in the thrust or the torque of a constant-incidence rotor are small.

Hence, by the use of a value of of $Q_\sigma' = 3.0$, which is representative of modern helicopters, the static-thrust variation of figure 11 may be used in equations (7) and (8) to determine the vertical velocities of approach to the ground. The result is shown in figure 12, which gives a set of specimen curves that are illustrative of the approximate solution of the problem. A more exact determination would, of course, require taking into account the small effect of velocity on thrust and torque.

Example

The following example illustrates the use of the curves of figure 12 for a helicopter rotor of 20-foot radius standing 10 feet off the ground when the aircraft is at rest:

Case I: To determine the permissible velocity of descent V_o for "automatic" landing without shock - that is, $V = 0$.

The value of Z/R at the ground is 0.50. For this value at

$$\frac{V}{V_o} = 0$$

$$\frac{V_o^2}{R} = 14.5$$

and $$V_o = \sqrt{14.5\ R}$$

$$= 17.0 \text{ feet per second}$$

Case II: To determine the velocity of impact for $V_o > 17.0$ feet per second

For

$$\frac{V_o^2}{R} = 19.2$$

$$\frac{V}{V_o} = 0.50$$

However, since $$V_o = \sqrt{19.2\ R}$$

$$= 19.6 \text{ feet per second}$$

$$V = 19.6 \times \frac{V}{V_o}$$

$$= 9.80 \text{ feet per second}$$

It should be noted that, for an increase of only 2.6 feet per second in V_o, the velocity of impact V changes from 0 to 9.8 feet per second, indicating that the automatic landing condition is somewhat critical.

Case III: To determine the behavior of this helicopter when $V_o < 17.0$ feet per second would require further investigation. It is evident that the machine would not reach the ground and might even perform one or two vertical oscillations before coming to the steady condition of hovering. No knowledge of the damping coefficient of this motion is available, however, and the actual behavior of the aircraft under such conditions cannot therefore be predicted with assurance.

REFERENCES

1. Küssner, Hans Georg: Helicopter Problems. T.M. No. 827, NACA, 1937.

2. Focke, H.: The Focke Helicopter. T.M. No. 858, NACA, 1938.

3. Platt, Haviland H.: The Helicopter: Propulsion and Torque. Jour. Aero. Sci., vol. 3, no. 11, Sept. 1936, pp. 398-405.

4. Betz, A.: The Ground Effect on Lifting Propellers. T.M. No. 836, NACA, 1937.

5. Knight, Montgomery, and Hefner, Ralph A.: Static Thrust Analysis of the Lifting Airscrew. T.N. No. 626, NACA, 1937.

6. Fagan, Robert H.: Vertical Ascent Analysis of the Lifting Airscrew. Georgia School of Technology thesis, 1940.

TABLE I

Ground-Effect Test Data for the Two-Blade Rotor

(σ = 0.0424)

	Z/R = 0.25		Z/R = 0.5		Z/R = 1.0	
θ (deg)	T_σ	Q_σ'	T_σ	Q_σ'	T_σ	Q_σ'
1	0.41	0.08	0.29	0.03	0.19	0.00
2	1.00	.35	.75	.24	.56	.19
4	2.21	1.03	1.87	1.00	1.52	1.03
6	3.41	2.16	3.13	2.29	2.69	2.49
8	4.20	3.47	3.93	3.57	3.52	3.75
10	4.55	4.20	4.31	4.24	3.92	4.52
12	5.36	6.57	5.25	6.42	5.01	6.66
14	6.00	8.50	6.01	9.12	5.84	9.15

	Z/R = 1.5		Z/R = 2.0	
θ (deg)	T_σ	Q_σ'	T_σ	Q_σ'
1	0.15	0.00	0.14	0.00
2	.48	.25	.47	.21
4	1.41	1.05	1.37	1.05
6	2.49	2.57	2.46	2.59
8	3.29	3.83	3.25	3.85
10	3.66	4.52	3.59	4.58
12	4.77	6.87	4.70	6.92
14	5.58	9.04	5.56	9.49

TABLE II

Ground-Effect Test Data for the Three-Blade Rotor

(σ = 0.0636

	Z/R = 0.25		Z/R = 0.5		Z/R = 1.0	
θ (deg)	T_σ	Q_σ'	T_σ	Q_σ'	T_σ	Q_σ'
1	0.25	0.05	0.16	-0.02	0.12	0.00
2	.60	.18	.43	.09	.33	.09
4	1.38	.51	1.09	.43	.89	.46
6	2.11	1.00	1.83	.96	1.55	1.02
8	2.83	1.77	2.62	1.83	2.31	1.95
10	3.69	3.35	3.60	3.50	3.41	3.67

	Z/R = 1.5		Z/R = 2.0	
θ (deg)	T_σ	Q_σ'	T_σ	Q_σ'
1	0.08	0.00	0.07	0.00
2	.26	.11	.25	.11
4	.79	.45	.75	.43
6	1.41	1.03	1.37	1.02
8	2.11	1.93	2.08	1.95
10	3.19	3.68	3.14	3.68

TABLE III

Ground-Effect Test Data for the Four-Blade Rotor

(σ = 0.0849)

	Z/R = 0.25		Z/R = 0.5		Z/R = 1.0	
θ (deg)	T_σ	Q_σ'	T_σ	Q_σ'	T_σ	Q_σ'
1	0.17	0.02	0.11	0.00	0.07	0.00
2	.40	.05	.28	.03	.20	.03
4	.95	.25	.73	.21	.57	.20
6	1.46	.52	1.24	.52	1.02	.53
8	2.02	.98	1.82	1.00	1.56	1.03
10	2.53	1.55	2.38	1.59	2.15	1.70

	Z/R = 1.5		Z/R = 2.0	
θ (deg)	T_σ	Q_σ'	T_σ	Q_σ'
1	0.05	0.01	0.05	0.00
2	.16	.00	.15	.03
4	.50	.20	.47	.19
6	.93	.53	.89	.52
8	1.42	1.03	1.38	1.02
10	1.99	1.70	1.93	1.68

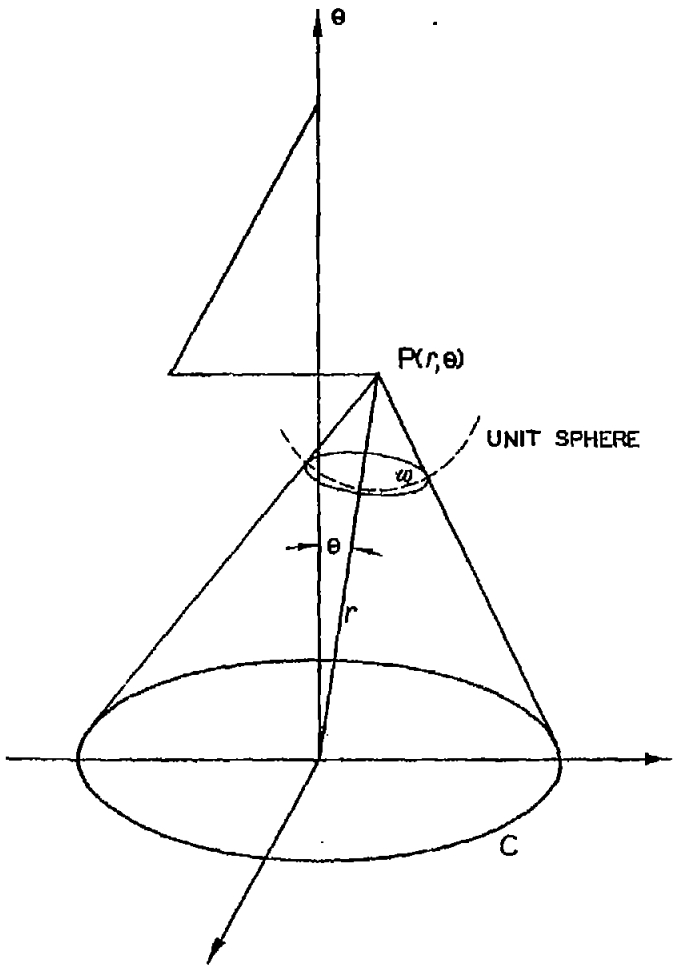

Fig. 3.

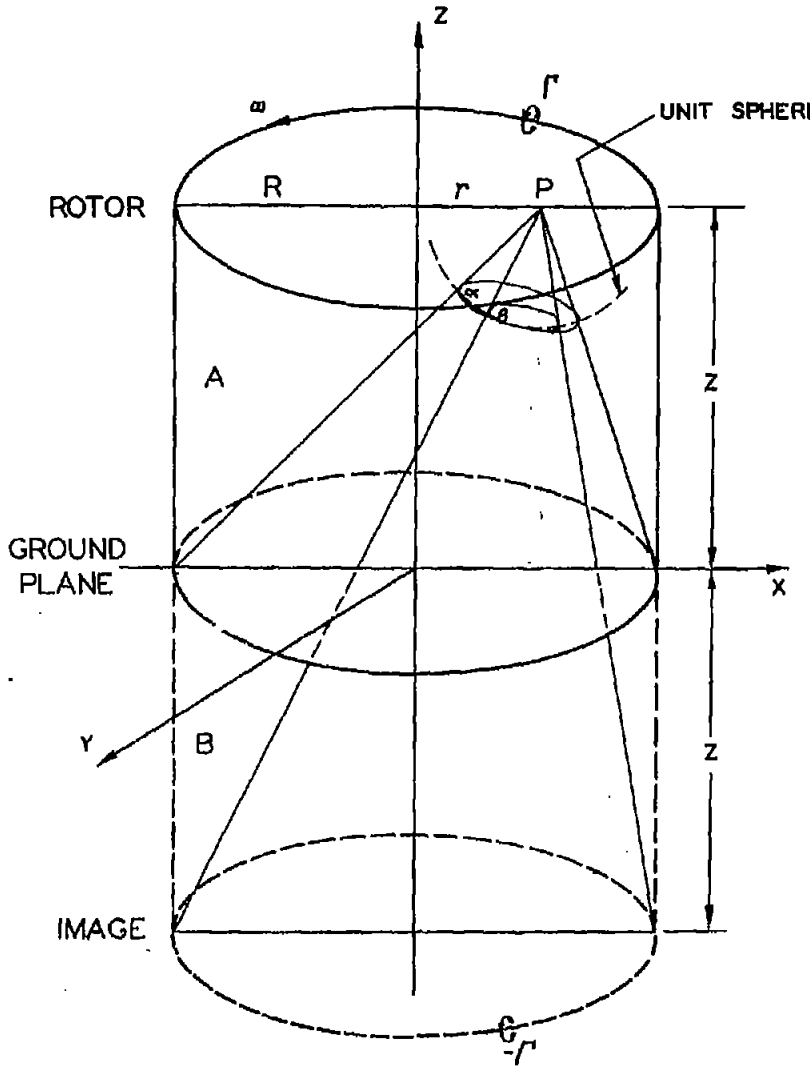

Fig. 1.

Vortex System for Ground Effect Analysis.

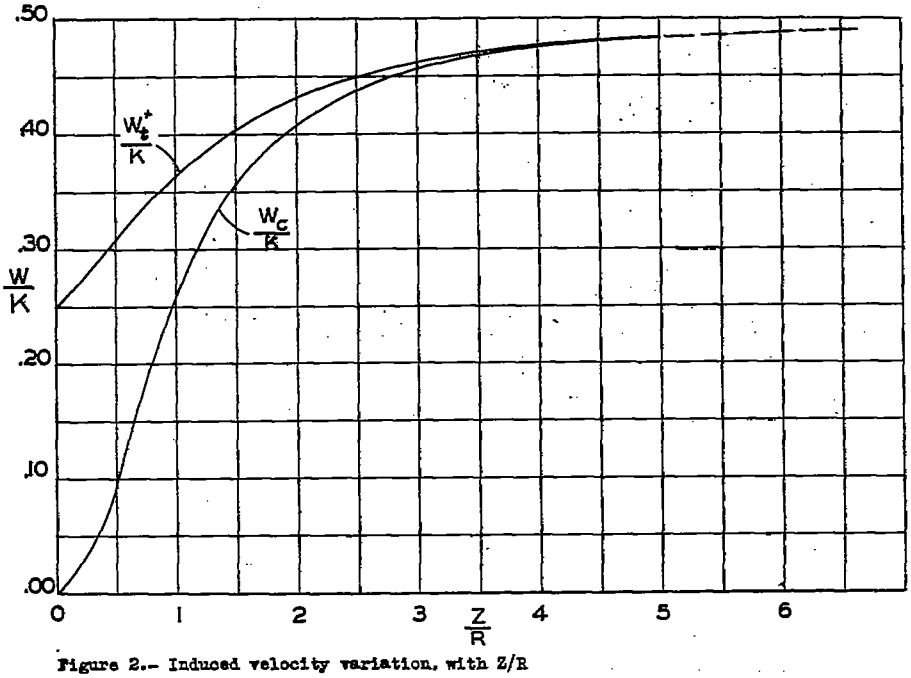

Figure 2.- Induced velocity variation with Z/R

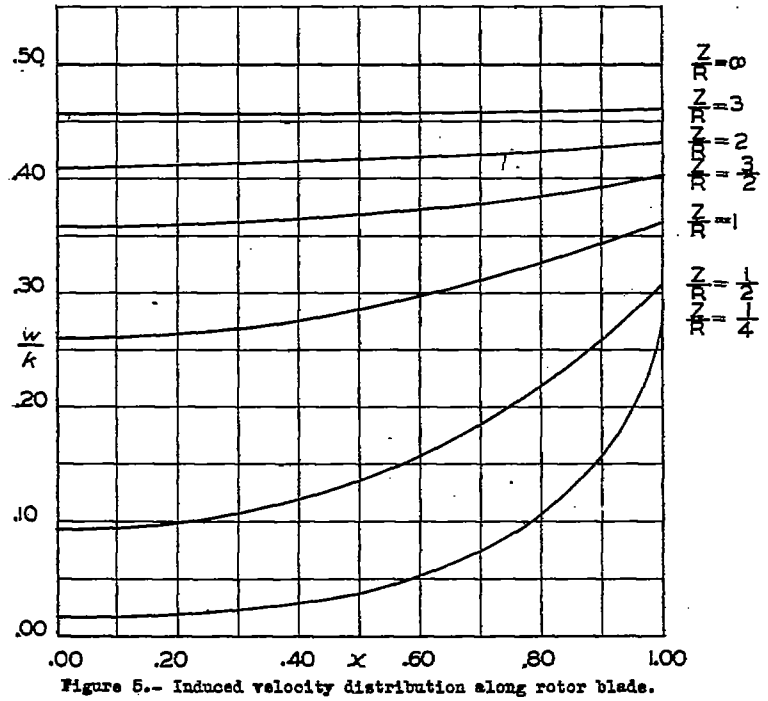

Figure 5.- Induced velocity distribution along rotor blade.

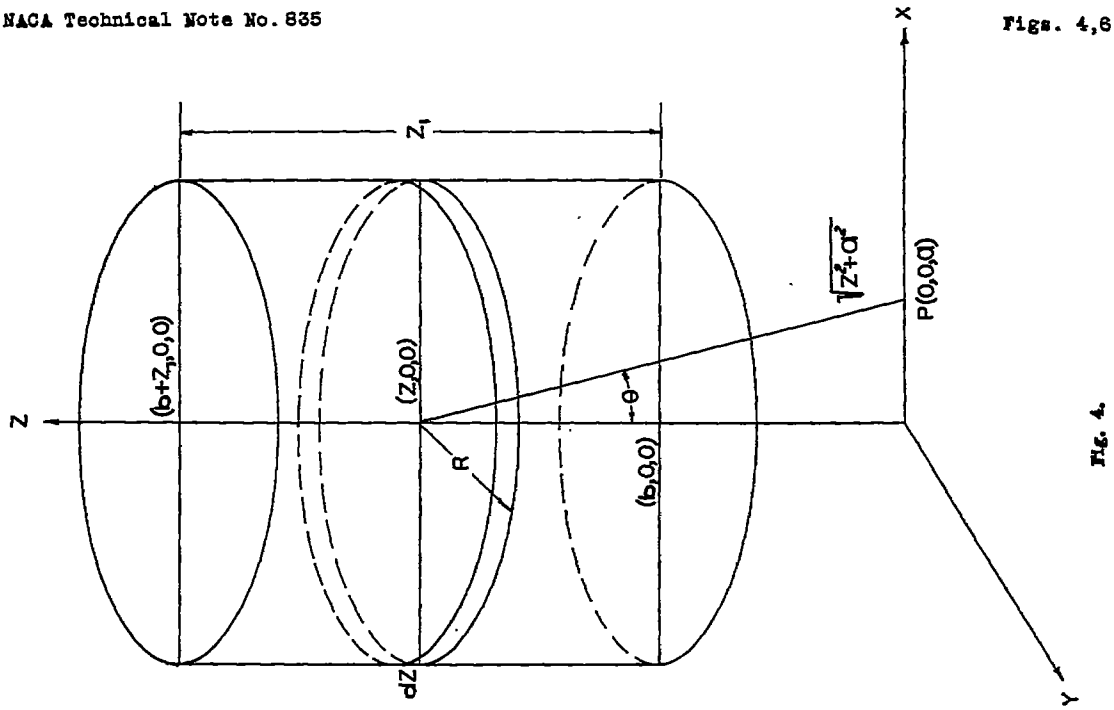

Fig. 4.

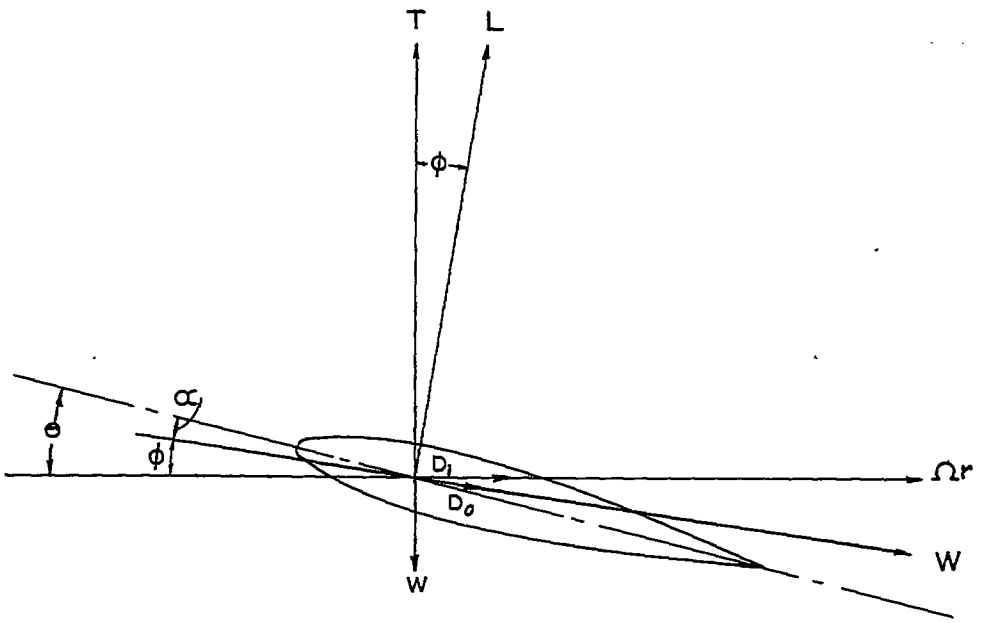

Fig. 6.

Force and Velocity Vectors for Blade Element.

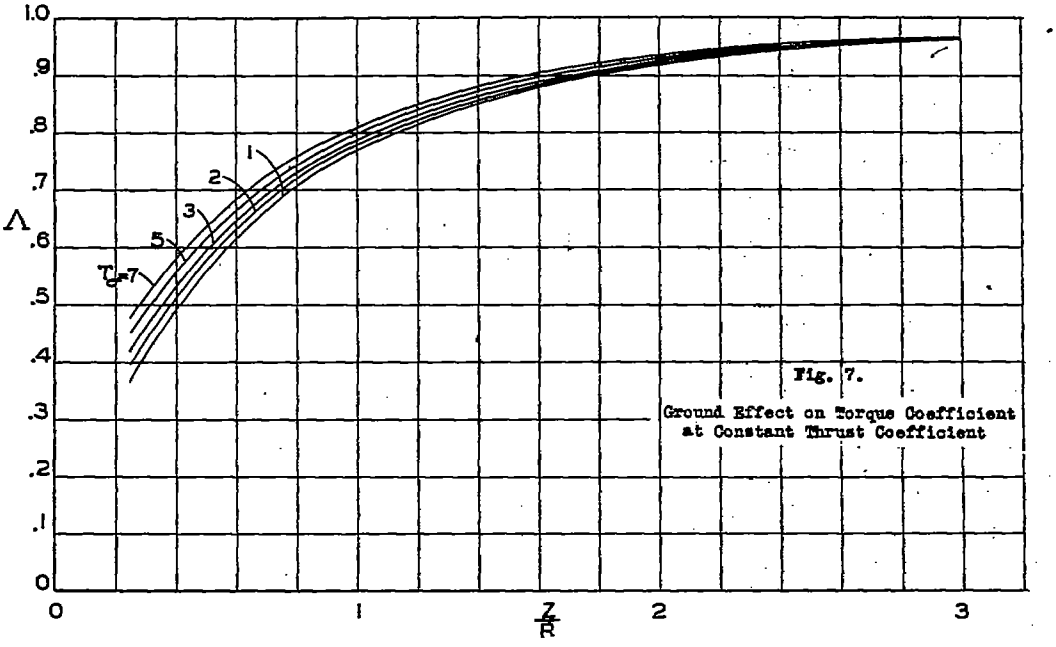

Fig. 7.
Ground Effect on Torque Coefficient at Constant Thrust Coefficient

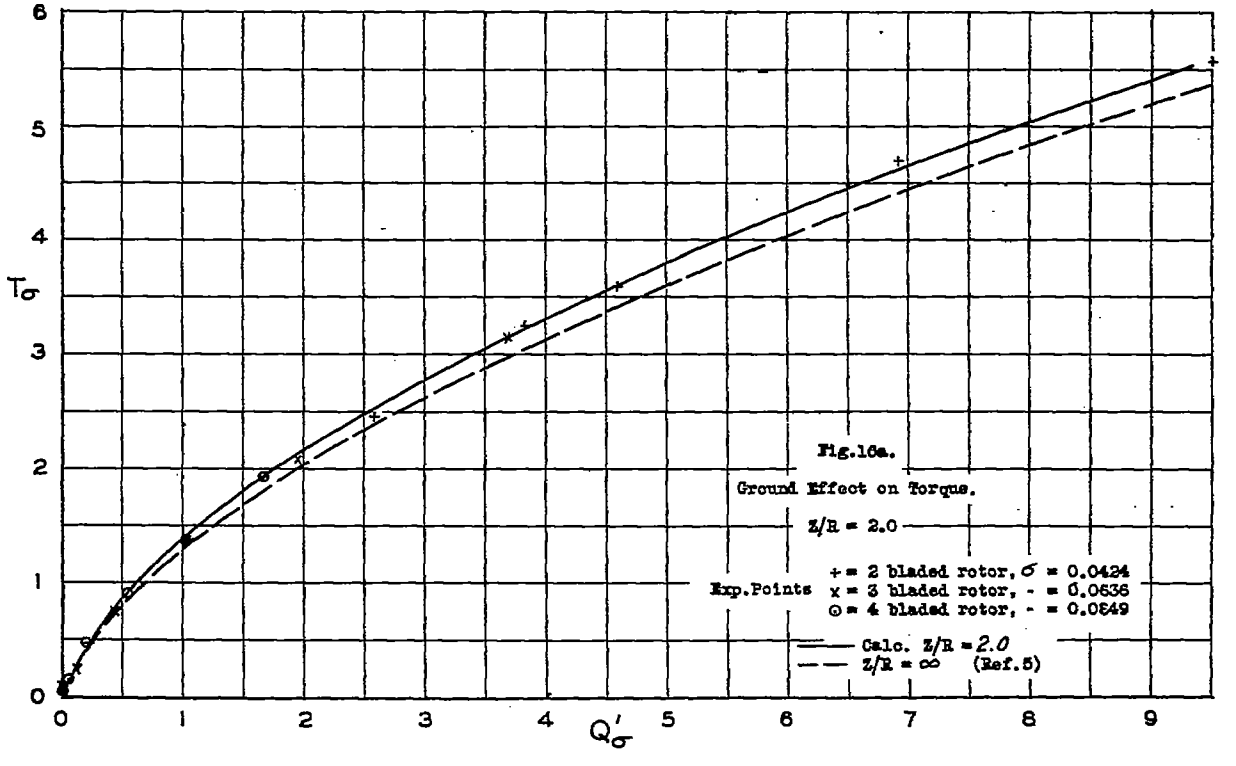

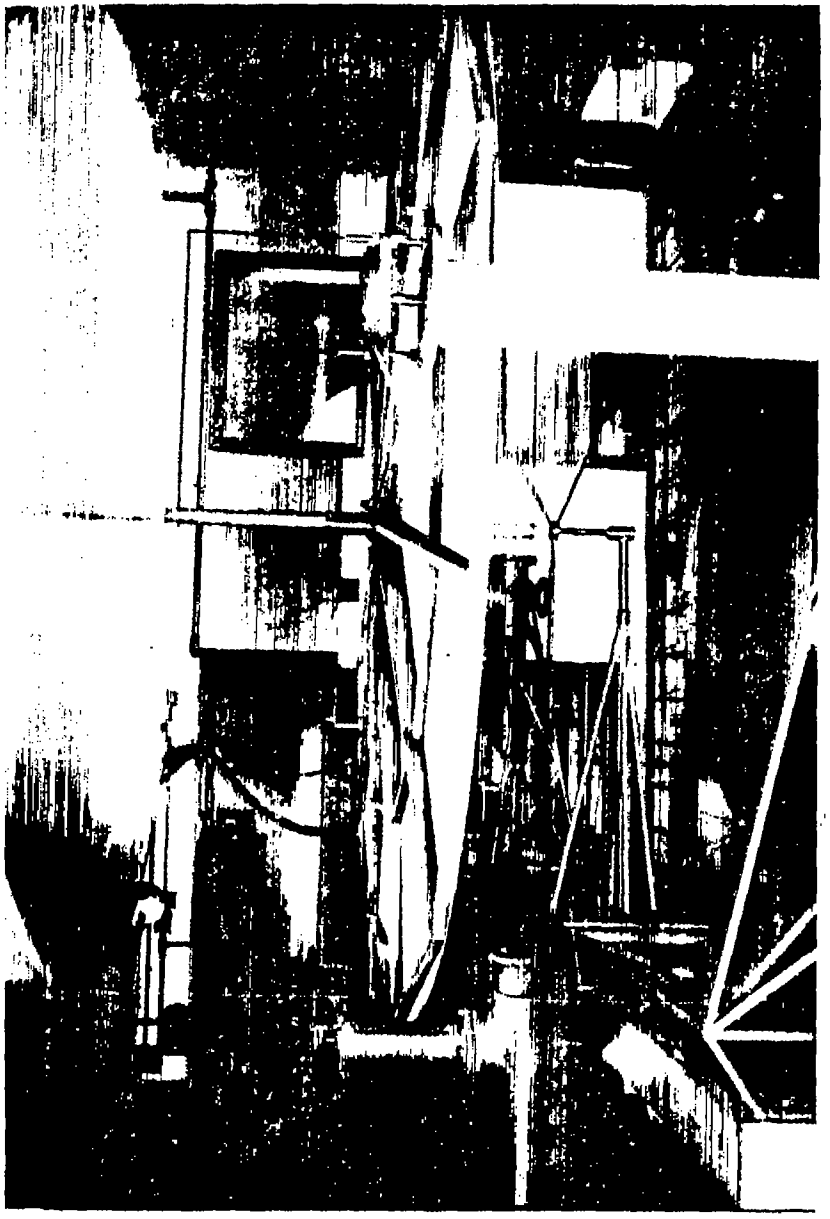

Figure 8.- Side view of ground plane mounted in 9-foot wind tunnel.

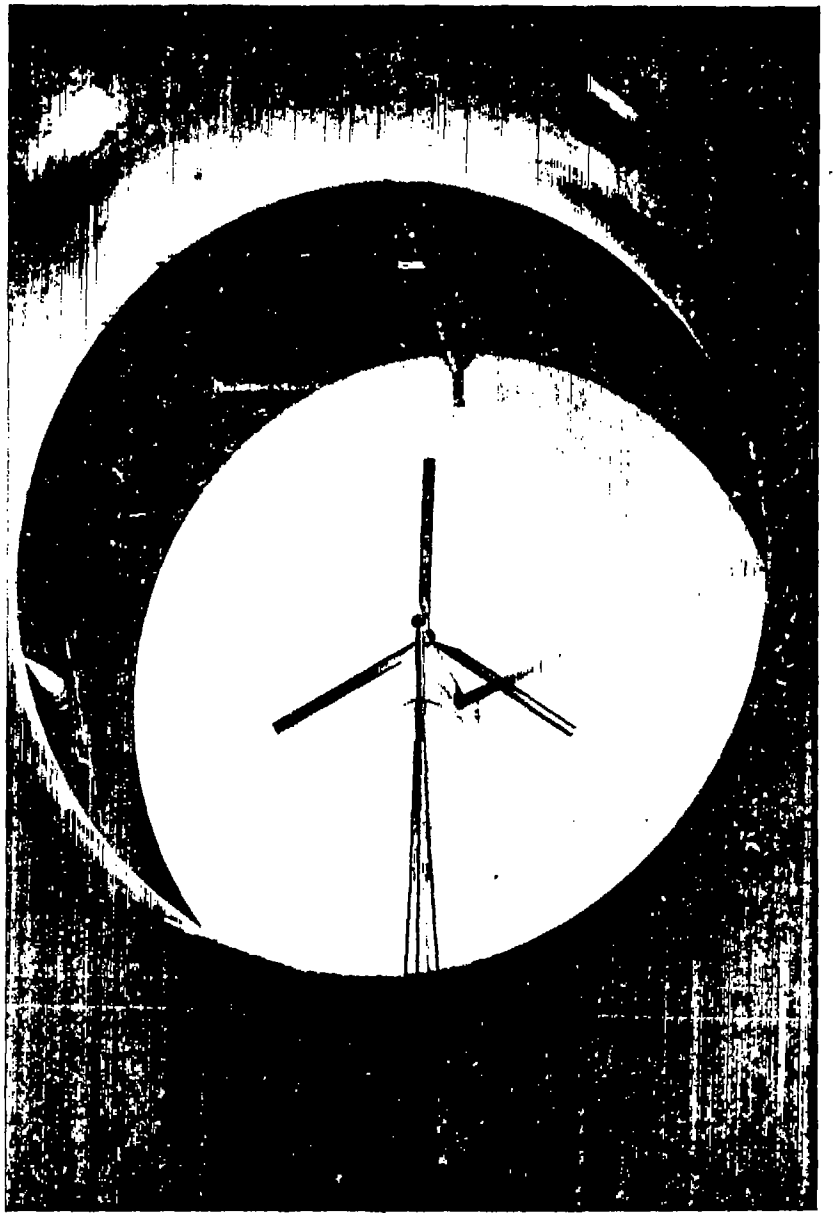

Figure 9.- Three-bladed rotor model and ground plane viewed from tunnel entrance cone.

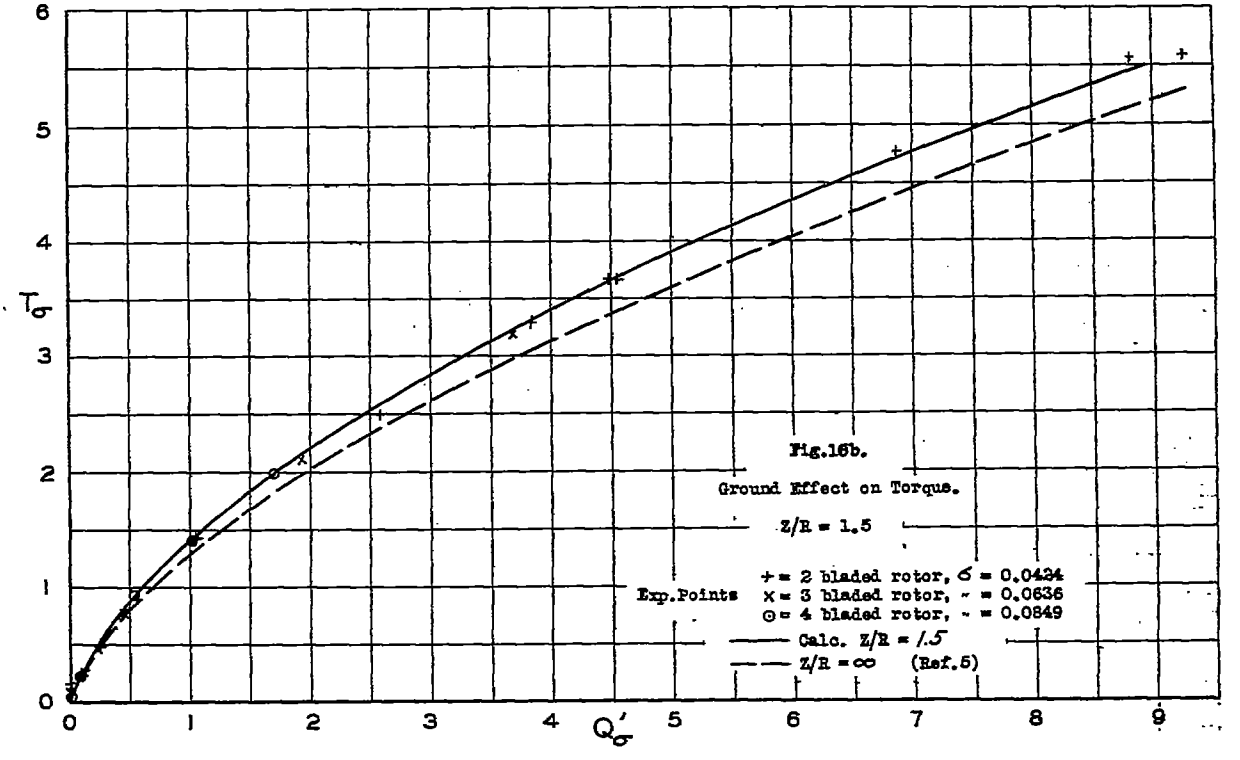

Fig.16b.
Ground Effect on Torque.
Z/R = 1.5

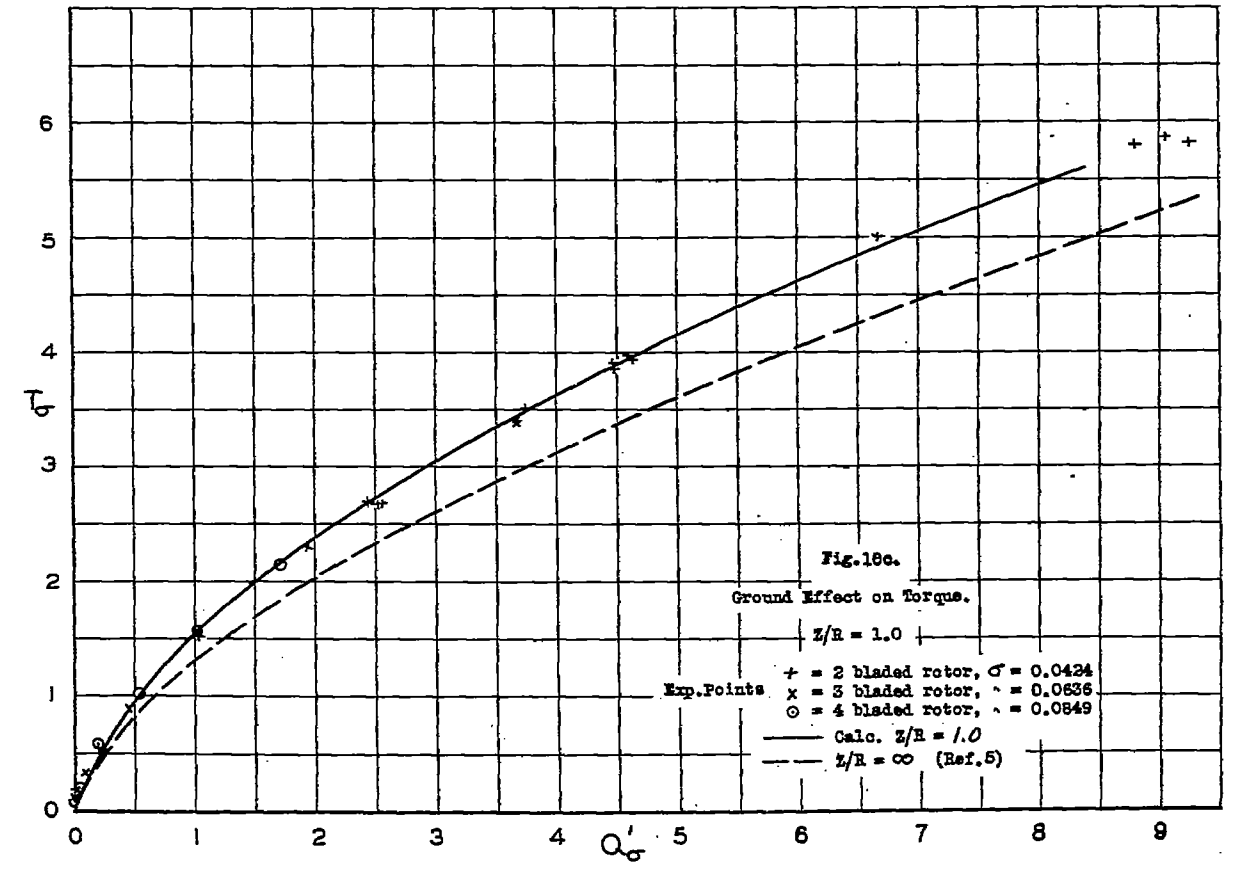

Fig.16c.
Ground Effect on Torque.
Z/R = 1.0

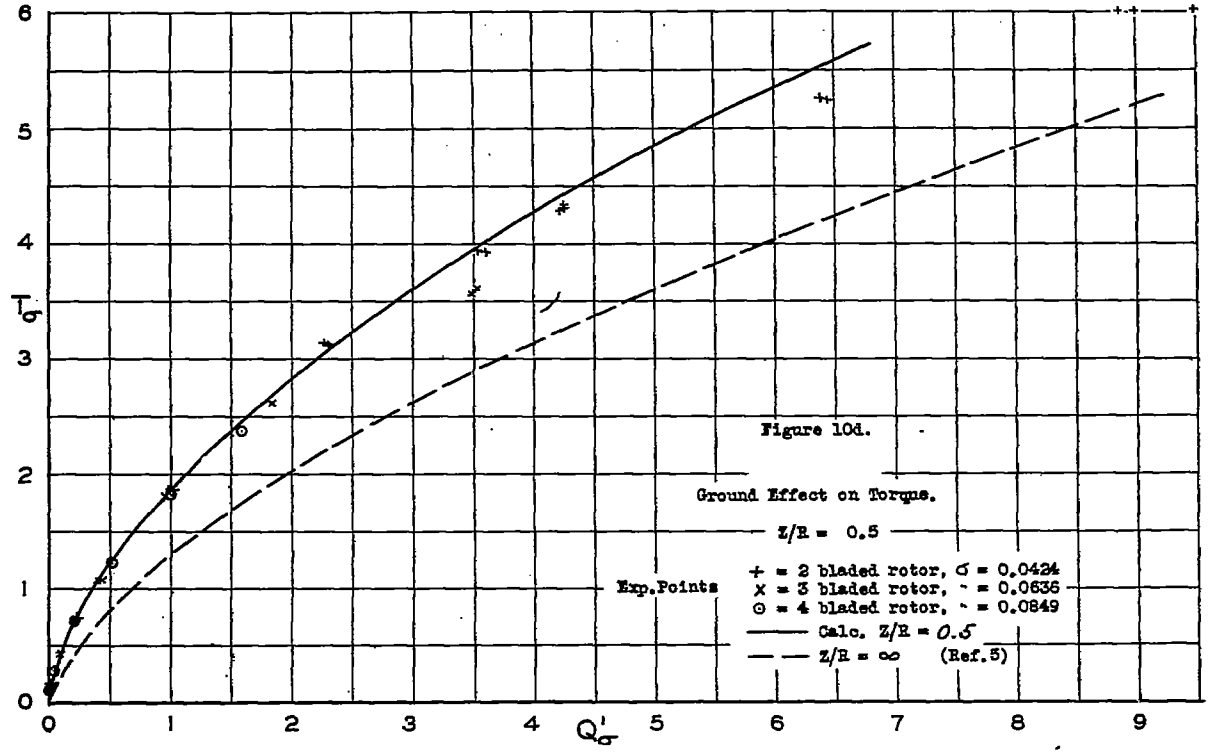

Figure 10d.

Ground Effect on Torque.

Z/R = 0.5

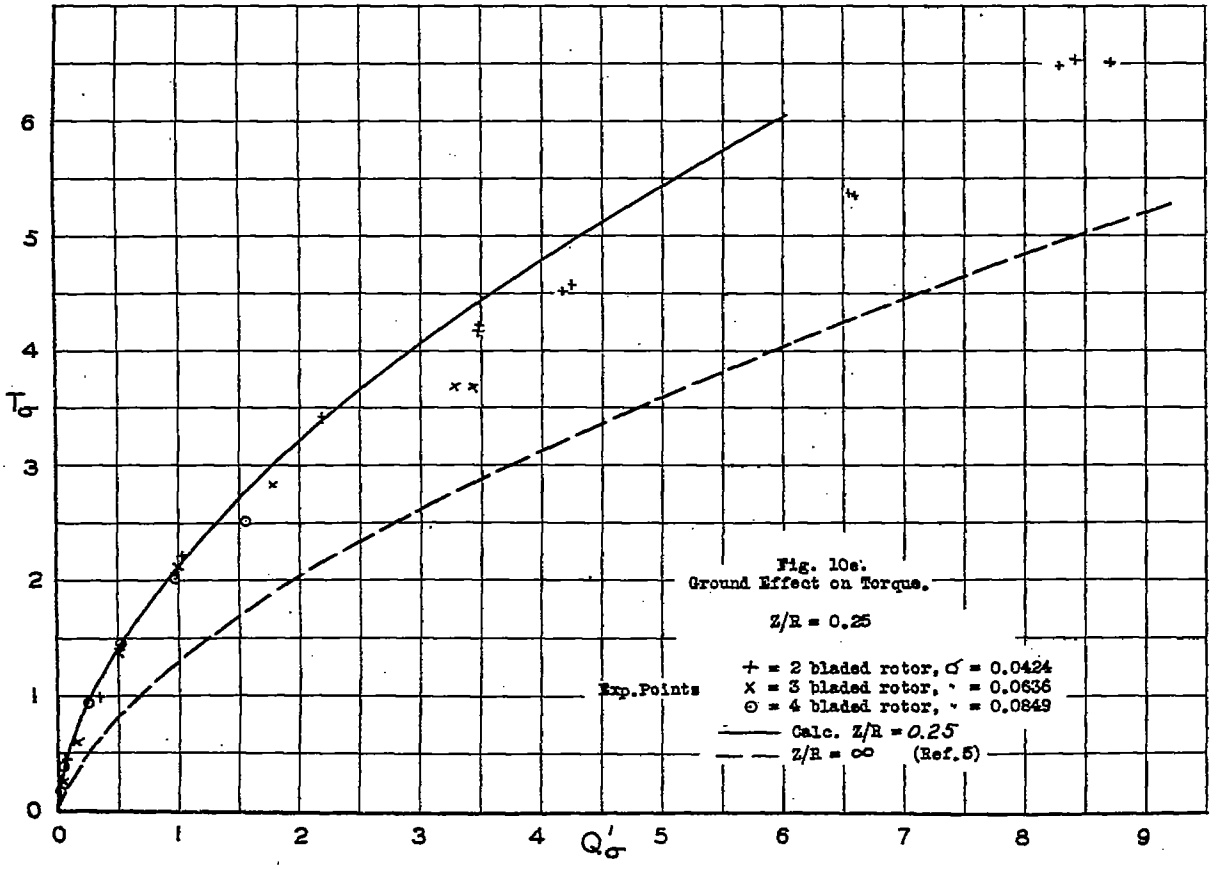

Fig. 10e.
Ground Effect on Torque.

Z/R = 0.25

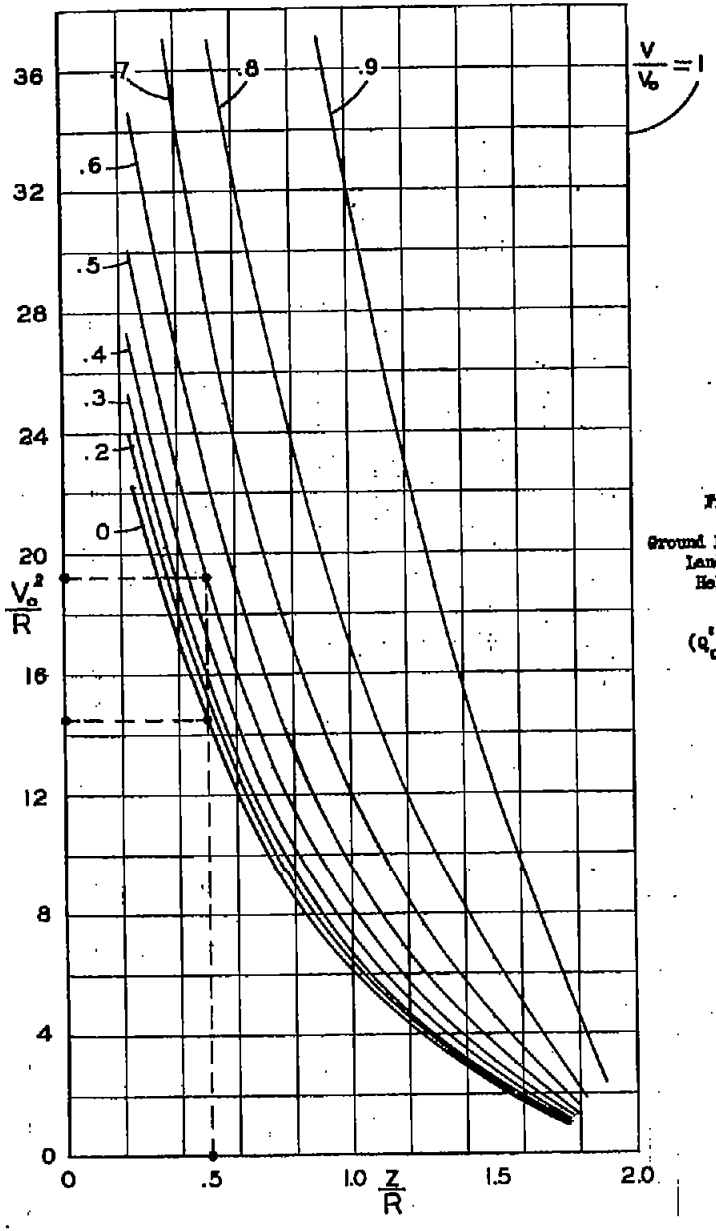

Fig. 12.

Ground Effect on the Landing of a Helicopter.

($\mu'_{\sigma}=3$)

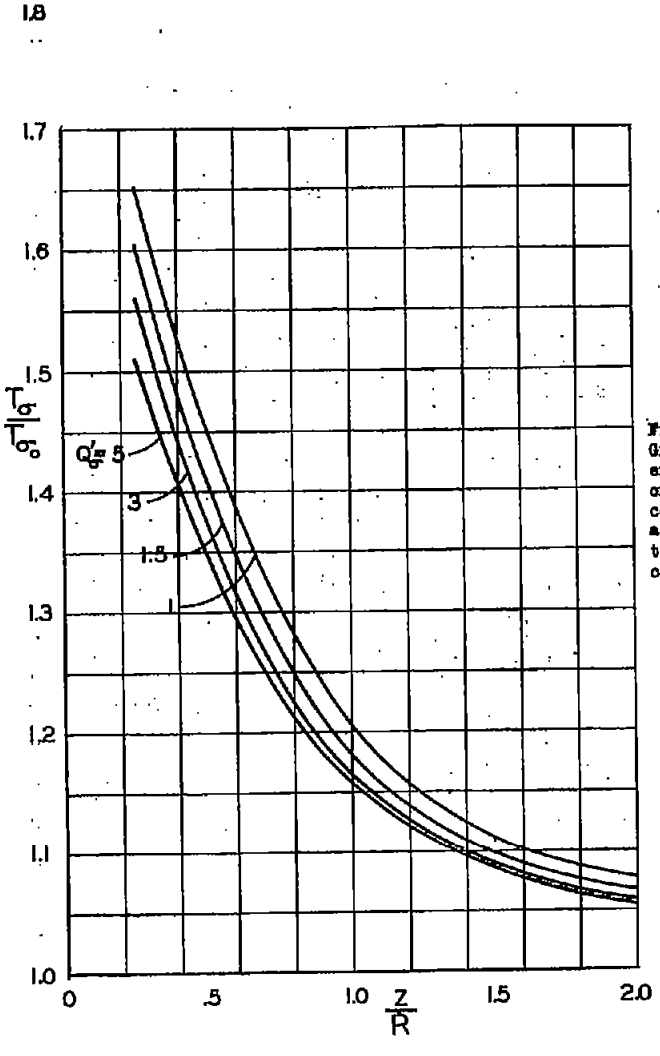

Figure 11.- Ground effect on thrust coefficient at constant torque coefficient.